Talanta 107 (2013) 133–139

Contents lists available at SciVerse ScienceDirect

Talanta

journal homepage: www.elsevier.com/locate/talanta

Luminescent ZnO quantum dots for sensitive and selective detection of dopamine

Di Zhao, Hongjie Song, Liying Hao, Xing Liu, Lichun Zhang, Yi Lv*

Key Laboratory of Green Chemistry & Technology, Ministry of Education, College of Chemistry, Sichuan University, Chengdu, Sichuan 610064, China

ARTICLE INFO

Article history:
Received 5 October 2012
Received in revised form
2 January 2013
Accepted 4 January 2013
Available online 11 January 2013

Keywords:
APTES-capped ZnO QDs
Dopamine
Fluorescence quenching
Fluorescent probe

ABSTRACT

Water-soluble and luminescent ZnO quantum dots (QDs) capped by (3-aminopropyl) triethoxysilane (APTES) are environment-friendly with strong photoluminescence (max. wavelength: 530 nm). Interestingly, it was found that the fluorescence could be quenched by dopamine (DA) directly. On the basis of above, a novel ZnO QDs based fluorescent probe has been successfully designed to detect DA with high selectivity and sensitivity. Moreover, the possible fluorescence quenching mechanism was proposed, which showed that the quenching effect may be caused by the electron transfer from ZnO QDs to oxidized dopamine–quinone. Under optimum conditions, the relative fluorescence intensity was linearly proportional to the concentration of DA within the range from 0.05 to 10 μM, with the detection limit down to 12 nM ($n=3$). Also, the selectivity experiment indicated the probe had a high selectivity for DA over a number of possible interfering species. Finally, this method was successfully used to detect DA in serum samples with quantitative recoveries (99–110%). With excellent selectivity and high sensitivity, it is believed that the ZnO QDs based fluorescent probe has a potential for the practical application in clinical analysis.

1. Introduction

In recent years, much attention has been paid to ZnO QDs, thanks to their unique optical and electrical properties [1–4]. As semiconductor QDs, ZnO QDs have high quantum yield, quantum size effects, broad absorption spectrum, and narrow emission spectrum [5,6]. Moreover, based on the direct band gap (3.37 eV) and large excitation binding energy (60 meV), ZnO QDs act as one of the brightest emitters among available wide band gap semiconductors [7,8]. ZnO QDs have shown wide applications in many fields, such as drug delivery, live cell imaging, UV photodetector, gas sensors, solar cells where their prominent optical and electrical properties become one of the focus issues [9–17]. On the other hand, compared with traditional semiconductor QDs (e.g., CdS, CdTe, CdSe), ZnO QDs are environment-friendly, less expensive and biocompatible to the biological systems [18,19], and have inspired great interest in biological labeling and biosensing. Further, the excellent fluorescent properties of ZnO QDs prompted us to apply them as fluorescence probe for biological and chemical detection.

Dopamine (DA), as one of important catecholamine neurotransmitter and derived from the amino acid tyrosine, plays a crucial role in normal homeostasis and clinical diagnosis. It is important to detect DA because the abnormal content of DA may result in several diseases and neurological disorders, such as schizophrenia, Parkinson's and Alzheimer's diseases [20–23]. Up to now, a lot of methods have been developed to detect DA such as electrogenerated chemiluminescence, electrochemical, capillary electrophoresis, colorimetry, high performance liquid chromatography, flow-injection analysis and fluorescent method [24–30]. Among these methods, more attentions have been paid recently to fluorescent method due to its simplicity and low detection limit. For example, Imato et al. reported a simple fluorometric assay for DA using a calcein blue-Fe^{2+} complex fluorophore [31]; Yan et al. described a GO-based label-free near-infrared fluorescent biosensor for DA [32]; Zhang et al. demonstrated the use of organic nanowire/Ag nanoparticle hybrid for the detection of DA based on fluorescence-enhancement [33]. However, detection of DA in biological matrixes usually suffers from a series of interference caused by other aromatic acids, amino acids, particularly ascorbic acid (AA), and uric acid (UA). Therefore, it is still a challenge for development of the fluorescent method for the determination of DA with high selectivity and sensitivity.

In this work, we prepared water-soluble and luminescent ZnO quantum dots (QDs) capped by APTES (APTES-capped ZnO QDs) through two-step procedure and found the fluorescence of ZnO QDs could be selectively quenched by DA directly, accordingly, a

* Corresponding author. Tel./fax: +86 28 8541 2798.
E-mail address: lvy@scu.edu.cn (Y. Lv).

0039-9140/$ - see front matter © 2013 Elsevier B.V. All rights reserved.
http://dx.doi.org/10.1016/j.talanta.2013.01.006

novel label-free ZnO QDs based fluorescent probe was developed for sensitive and selective detection of DA in biological fluids. The proposed method had many advantages, such as high sensitivity, good selectivity, wide linear range, simple and fast determination procedure, safe operation, and little equipment investment. Most notably, ZnO QDs without any heavy metal ions made the fluorescent probe more eco-friendly. Thus, the ZnO QDs based fluorescent probe for DA exists potential applications in the clinical diagnosis, etiology, and prognosis.

2. Experimental

2.1. Chemicals and materials

All the reagents were analytical grade and used without further purification. Potassium hydroxide (KOH), ethanol absolute and ethyl acetate were obtained from Chengdu Kelong Chemical Reagent Co. Ltd. (Chengdu, China). Zinc acetate dihydrate ($Zn(OAc)_2 \cdot 2\,H_2O$) was obtained from Tianjin Kermel Chemical Reagent Co. Ltd. (Tianjin, China). Dopamine hydrochloride was purchased from Adamas Reagent Co. Ltd. (3-aminopropyl) triethoxysilane (APTES) was purchased from Aladdin Chemistry Co. Ltd. Ultrapure water (18.2 MΩ cm) obtained from a water purification system (ULUPURE, Chengdu, China) was used throughout this work.

2.2. Apparatus and measurements

All fluorescence measurements were obtained with a F-7000 fluorescence spectrophotometer (Hitachi Co., Tokyo, Japan). The UV–vis absorption spectra of ZnO QDs, DA and ZnO QDs–DA complex in the region of 200–800 nm were recorded by a U-2910 UV–vis spectrophotometer (Hitachi Co., Tokyo, Japan). The Fourier transform Infrared spectra (FTIR) were carried out on a Nicolet IS-10 FTIR Spectrometer (Thermo Inc., America) with KBr pellets. The transmission electron microscope (TEM) and high-resolution transmission electron microscopy (HRTEM) images of APTES-capped ZnO QDs were obtained from a Tecnai G^2 F20 S-TWIN transmission electron microscope at an accelerating voltage of 200 kV (FEI Co., America). The powder X-ray diffraction patterns (XRD) were recorded with an X' Pert Pro X-ray diffractometer (Philips, Netherlands).

2.3. Preparation of APTES-capped ZnO QDs

APTES-capped ZnO QDs was prepared by a two-step procedure, approximately according to the suggestions in the previous literature [18,34]. In the first step, the $Zn(OAc)_2$ solution was prepared by dissolving 1.0 mmol of $Zn(OAc)_2 \cdot 2\,H_2O$ in 100 mL ethanol. 3.0 mmol of KOH was dissolved in 8 mL of ethanol and kept in an ultrasonic bath for 40 min at room temperature. The obtained KOH solution was dropwise added to $Zn(OAc)_2$ solution followed by continuous stirring for 1.5 h under 25 °C. The ZnO QDs were precipitated by addition of ethyl acetate. After centrifugation, the precipitate was washed by absolute ethanol for three times to remove unreacted materials. The final particles were collected by centrifugation and redispersed in 20 mL of ethanol under agitation for further preparation.

In the second step, the ZnO QDs were capped with APTES by adding 0.05 M APTES ethanol solution (10 mL) to the as prepared 20 mL ZnO QDs solution dispersed in ethanol, then 0.40 mL of deionized water was quickly added under vigorous stirring. The reaction mixture was stirred for an hour at room temperature (25 °C). The product was obtained by ultracentrifugation with 8000 rpm for 10 min, and washed with absolute ethanol for three times. Finally, the precipitated nanocrystals were redispersed in deionized water or absolute ethanol for further study. This two-stage silanization has successfully introduced amino groups onto the ZnO QDs.

2.4. Sample collection and pretreatment

Two human serum samples were collected from healthy adult volunteers. All samples were subjected to a 100-fold dilution before analysis, and no other pretreatments were necessary.

2.5. Measurement procedures

The DA detection procedure by ZnO QDs was described as follows: 50 μL of QDs aqueous solution reacted with different concentrations of DA solution (concentration from 0.05 to 10 μM in deionized water). The mixture was diluted into 1.00 mL with deionized water and mixed thoroughly, and then incubated in a water bath at 40 °C for 20 min. After the mixture was cooled to room temperature, fluorescence measurements were performed at an excitation wavelength of 337 nm.

3. Results and discussion

3.1. Characterization of the APTES-capped ZnO QDs

The APTES-capped ZnO QDs showed a broad absorption at 330 nm in the ultraviolet region, and an emission peak at 530 nm under excitation of 337 nm (Fig. 1B). The broad bandwidth of 112 nm emission peak suggested that the luminescence of ZnO QDs was possibly due to surface trap effect [35]. The photograph of the ZnO QDs demonstrated the strong yellow emission (Fig. 1B). The XRD results indicated that ZnO QDs have hexagonal crystal structure which was consistent with the reported results [16] (Fig. 1C). The HRTEM image showed lattice fringes with distances of 0.282 nm corresponding to the inter-planer distances of the (1 0 0) planes of wartzite ZnO (Fig. 1A). TEM (Fig. 1A) and XRD peaks broadening analyses indicated the particle size of ZnO QDs was ca. 3–5 nm. The silane coating was not observed in the HRTEM image, indicated that the surface coating was very thin. The functional groups increased the water solubility and biocompatibility of ZnO QDs.

3.2. Fluorescence quenching of APTES-capped ZnO QDs colloids by DA

Addition of DA to the aqueous solution of QDs led to a significant quenching of the fluorescence of QDs without an obvious shift of the fluorescence emission peak. As shown in Fig. 2A, the fluorescence intensity of QDs decreased to 11% in the presence of 5 μM DA. In order to verify the function of APTES which capped on QDs surface by silanization, the same amount of DA was added to bare QDs aqueous solution, the fluorescence intensity only decreased to 67%, slight quenching of fluorescence compared to the former (shown in Fig. 2B). Control experiments showed that the quenches efficiency enhanced obviously after capped by APTES. This may be due to the hydrogen-bonding interaction between the amino-groups in APTES with DA.

The UV spectra and FTIR spectra can further confirmed the formation of the DA–QDs complex via noncovalent interactions. Fig. 3A showed the decrease in intensity and shift of the absorption maximum with the addition of DA. The absorption spectrum of QDs–DA complex showed characteristic band at 322 nm for QDs and at 286 nm for DA. The absorption peak of QDs blue shifted ca. 8 nm by comparing with free QDs, due to hydrogen bond interaction with DA, and subsequently the fluorescence of QDs was drastically quenched.

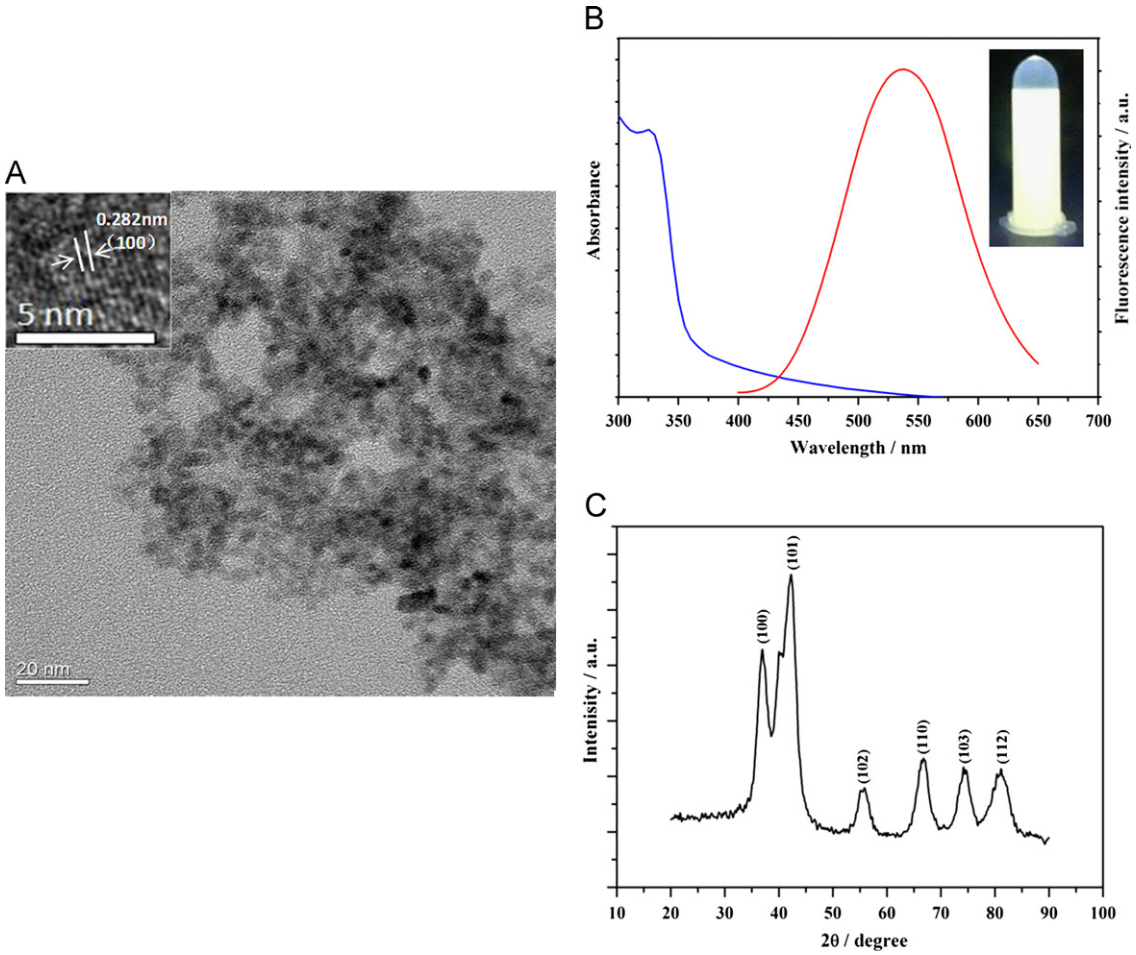

Fig. 1. (A) TEM image of APTES-capped ZnO QDs. Inset: HRTEM image (top-left corner). (B) UV–vis-near-IR absorption spectrum of DA (blue), fluorescence emission spectrum of ZnO QDs (red). Inset: photograph of ZnO QDs solution under UV light. (C) XRD patterns of APTES-capped ZnO QDs. (For interpretation of the references to colour in this figure legend, the reader is referred to the web version of this article.)

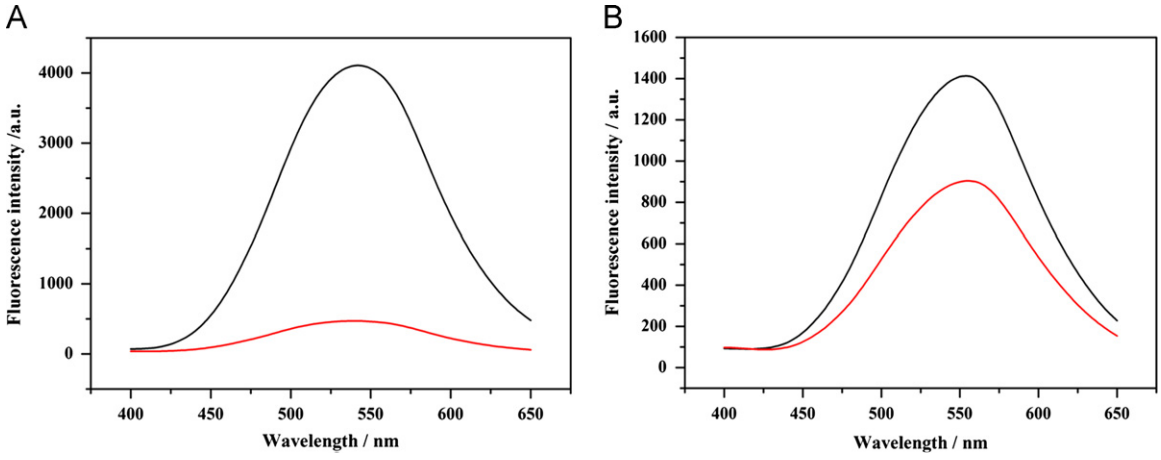

Fig. 2. (A) Fluorescence emission spectra of APTES-capped ZnO QDs (black), and the mixture of APTES-capped ZnO QDs and 5 μM DA (red). (B) Fluorescence emission spectra of ZnO QDs without capped by APTES (black), and the mixture of bare ZnO QDs and 5 μM DA (red). (For interpretation of the references to colour in this figure legend, the reader is referred to the web version of this article.)

As shown in Fig. 3B, the absorption peak at 3402 cm^{-1} could be attributed to the stretching vibration of $-NH_2$. The peak at 2900 cm^{-1} was the typical stretching vibration of $-CH_2-$. The peak at about 1481 cm^{-1} was the bending stretching of N–H, the observation of a broad absorption peak at 1111 cm^{-1} was corresponding to the Si–O vibration. A prominent absorption peak was observed at 439 cm^{-1} corresponding to the Zn–O stretching vibration. For DA, the characteristic peak at 3344 cm^{-1} was corresponding to the $-NH_3^+$ vibration stretching, the bands at 1616 and 1500 cm^{-1} were the stretching vibration of C=C in the benzene ring, and –OH vibration stretching of diols, respectively. As observed, compared with the spectra of QDs and DA, there was no new peak appeared in the spectrum of the QDs–DA complex. However, both the bending vibration peak and

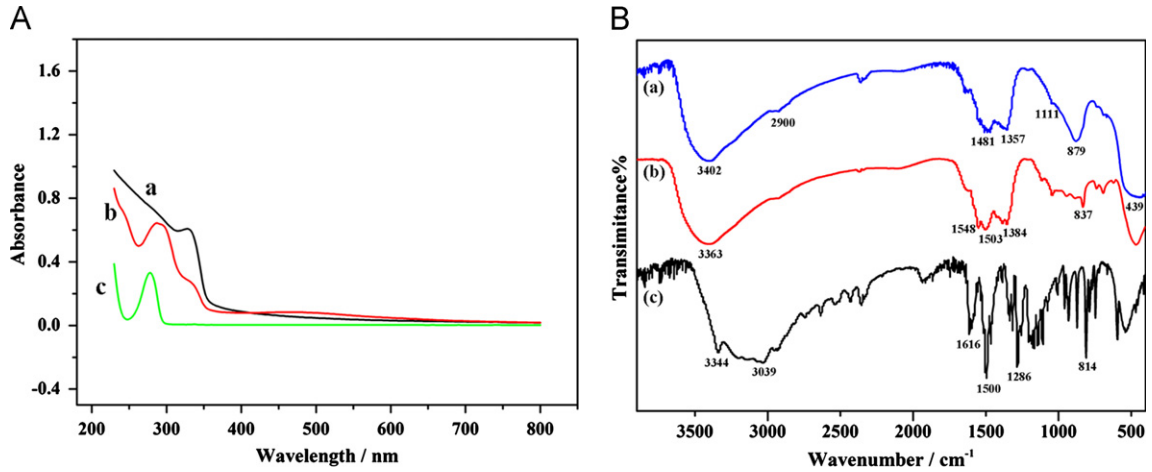

Fig. 3. (A) UV spectra of ZnO QDs (a), ZnO QDs–DA complex (b), and the DA (c). (B) FTIR spectra of ZnO QDs (a), ZnO QDs–DA complex (b), and the DA (c).

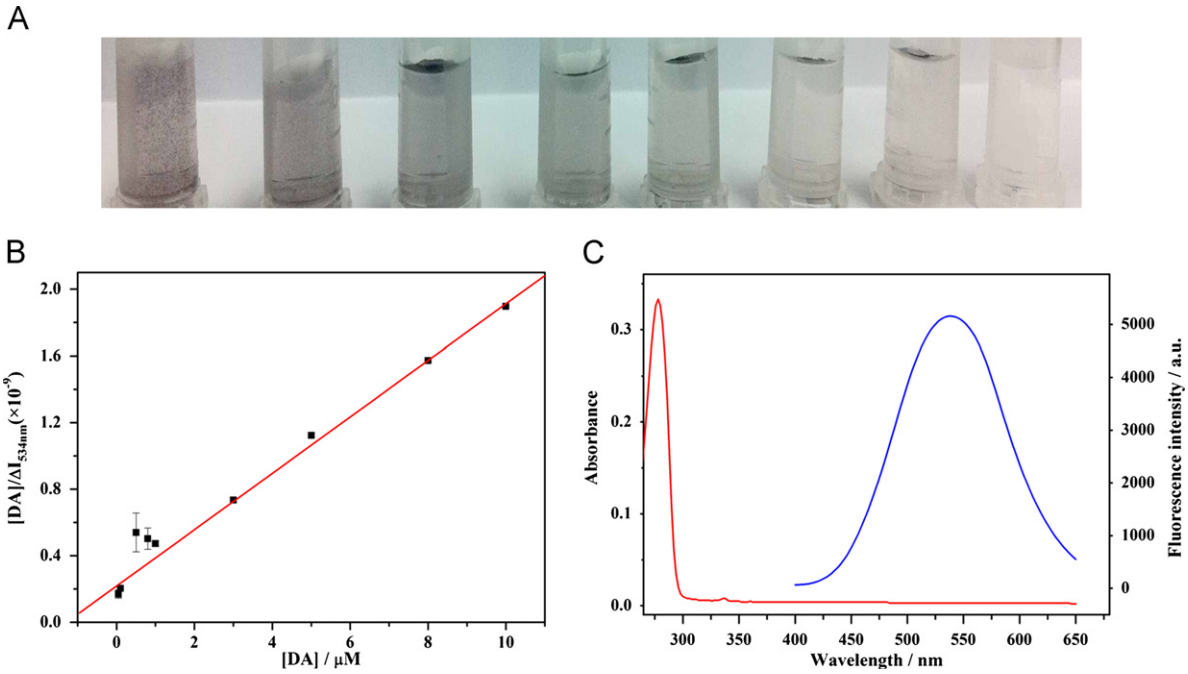

Fig. 4. (A) The corresponding color change of QDs interaction with different concentrations of DA. (B) Plot of [DA]/ΔI against [DA], showing a linear fit to the Langmuir adsorption isotherm. (C) UV–vis-near-IR absorption spectrum of DA (red), and fluorescence emission spectrum of QDs (blue). (For interpretation of the references to colour in this figure legend, the reader is referred to the web version of this article.)

stretching vibration peak of N–H broaden, which could be attributed to the hydrogen-bonding interaction of the amino groups in DA with QDs.

The Fig. 4A showed the corresponding color change of QDs interaction with different concentrations of DA in water. As the concentrations of DA increased, the color of the mixture became darker, and turned into atropurpureus finally. In the meantime, some small particles occurred and were observed even by naked eyes. The phenomenon of the aggregation of QDs was caused through the binding of DA and functional QDs. That is, the DA was adsorbed on QDs surface, thereby the fluorescence was quenched. To confirm the efficient adsorption process, the adsorption curve was investigated. The results showed the adsorption of DA molecules onto the QDs surface followed the Langmuir adsorption isotherm:

$$\frac{[DA]}{\Delta I} = \frac{[DA]}{\Delta I_{max}} + \frac{K_d}{\Delta I_{max}}$$

where K_d was the dissociation constant of the ZnO QDs–DA complex and ΔI_{max} was the fluorescence change at saturation. The K_d was estimated to be 1.3×10^{-6} M from the Langmuir adsorption isotherm in Fig. 4B. All the above results indicated that DA molecules were adsorbed onto the QDs surface via noncovalent interactions.

3.3. Study on the quenching mechanism

Recently, many researchers have focused on the applications of QDs for the development of sensing systems based on the changes of fluorescence intensity because of the fluorescence resonance energy transfer (FRET) [36], electron transfer (ET) [32], or other interactions occurring at the QDs surface [37]. From the UV spectra and FTIR spectra, the possibility of surface reaction could be ruled out for the formation of DA–ZnO QDs complex via noncovalent interactions. Meanwhile, there was no overlap between the absorption spectrum of DA and the emission spectrum of QDs, excluding FRET as a possible mechanism for QDs fluorescence quenching (Fig. 4C). Thus, the quenching effect presumably results from the effective electron transfer that occurred between QDs and DA. Because of the redox activity of dopamine, we attributed these findings to electron

transfer interactions between QDs and mainly two forms of dopamine: the reduced dopamine (electron donors) and the oxidized dopamine-quinone (electron acceptors). However, in this work, all experiments operated under alkalescent environment (pH 7.0–8.0). As we all know, DA can easily be oxidized by ambient O_2 in alkaline solution, and some studies showed quinones (oxidized dopamine) to be electron acceptors for QDs [38–41]. Therefore, the quenching mechanism of our fluorescent probe was presented in Fig. 5. When DA solution sample was added into the detection system, the DA molecules were adsorbed on QDs surface due to the strong non-covalent interactions such as electrostatic interaction and hydrogen bonding, and then the electron transfer from photoexcited QDs to oxidized dopamine–quinone, resulting in fluorescence quenching of QDs. The quenching reaction may be a static quenching.

The fluorescence quenching of APTES-capped ZnO QDs by different concentrations of DA was shown in Fig. 6A. As the concentration of DA increasing, the quenching of the QDs was enhanced. The Fig. 6B showed the change of the fluorescence intensity (ΔI) of QDs at 530 nm was of DA concentration ([DA]) dependence. ΔI increased linearly at low concentrations of DA and then gradually leveled off at higher concentrations of DA.

Moreover, the fluorescence quenching caused by DA was well described by the Stern–Volmer equation:

$$\frac{I_0}{I} = 1 + Ksv[DA]$$

where I_0 and I were the fluorescence intensity in the absence and presence of quencher (DA), respectively. K_{SV} was the Stern–Volmer constant representing the affinity between fluorophore and quencher. The plot of I_0/I at 530 nm against [DA] showed a linear range from 0.05 to 10 μM with a K_{SV} value of 5.5×10^5 M^{-1}, and the correlated coefficient 0.996 could also be acquired (inset in Fig. 6A).

3.4. Selectivity

Along with the sensitivity requirement, high specificity is crucial in most scenarios especially in real sample detections. To verify the

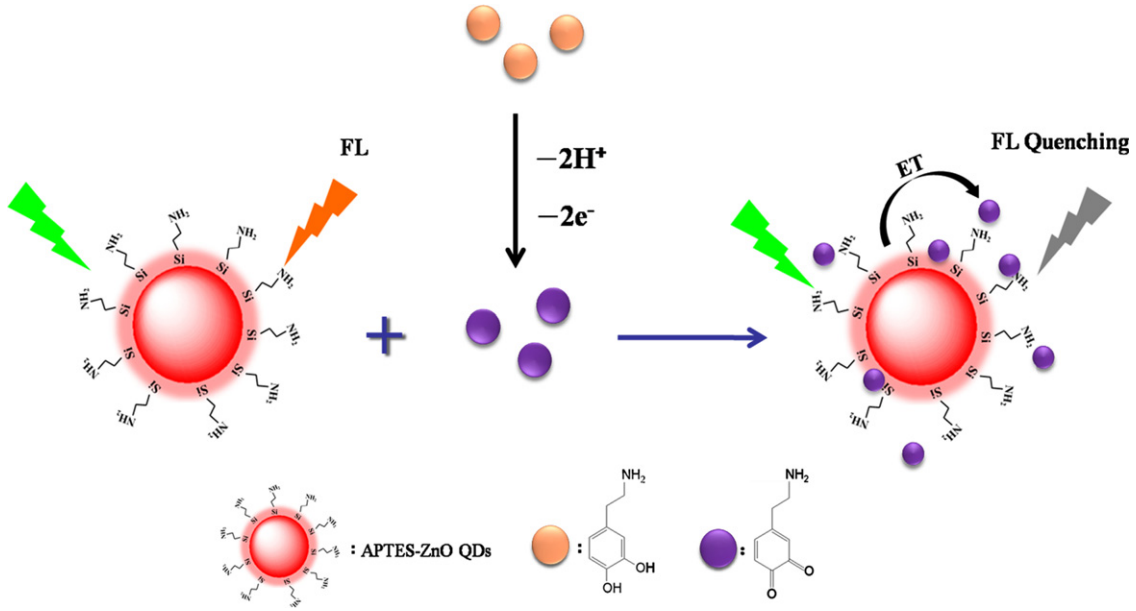

Fig. 5. Schematic illustration of the developed ZnO QDs-based fluorescent probe for DA.

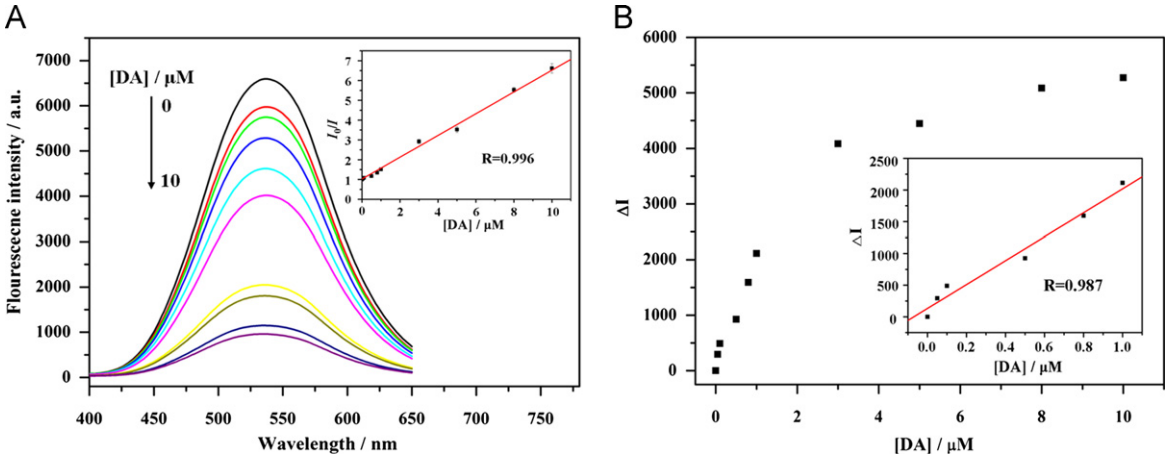

Fig. 6. (A) Emission spectra of 50 μL QDs with different concentrations of DA in aqueous solution (0, 0.05, 0.1, 0.5, 0.8, 1, 3, 5, 8 and 10 μM). The inset displays plots of the relative fluorescence intensity of QDs versus the concentration of DA. (B) Plot of the emission intensity changes at 530 nm against the DA concentration. Inset: expanded linear region of the calibration curve.

performance of the APTES-capped ZnO QDs as a DA probe in real samples, interferences from common molecules present in human blood serum were tested. As shown in Fig. 7, besides DA, the effect of 23 other kinds of biomolecule (amino acid, glucide and so on), including uric acid (UA), ascorbic acid (AA), serine (Ser), histidine (His), alanine (Ala), cysteine (Cys), lysine (Lys), glycine (Gly), valine (Val), leucine (Leu), arginine (Arg), tyrosine (Tyr), proline (Pro), asparagine (Asn), methionine (Met), homocysteine (Hcy), phenylalanine (Phe), glucose, lactose, sucrose, fructose (Fru), human serum albumin (HSA), and creatinine (Cr) were investigated. All of them had no obvious effects on the fluorescence emission. Particularly, AA and UA, which have similar electrochemical property to DA, did not affect the fluorescence of QDs. It turned out that the developed ZnO QDs based fluorescent probe offers high selectivity for DA because of strong noncovalent interactions between APTES-capped ZnO QDs and DA.

The developed ZnO QDs based label-free fluorescent probe was employed for selective and sensitive detection of DA in human serum sample. The recoveries of the DA in serum were also calculated and shown in Table 1. DA was added into these serum samples, and an appropriate amount of the sample solution was again detected. The recoveries of DA were found to be in the range of 99–110%. The RSD was between 0.5% and 4.0%. Moreover, there was negligible fluorescence background at 530 nm under excitation of 337 nm in serum samples. Table 2 shows the comparison of different analytical methods for DA detection, suggesting the proposed method exhibited a wider liner range, better detection limit, higher sensitivity and selectivity for DA. It proved that the ZnO QDs based fluorescent probe is appropriate for the practical application in clinical analysis of DA.

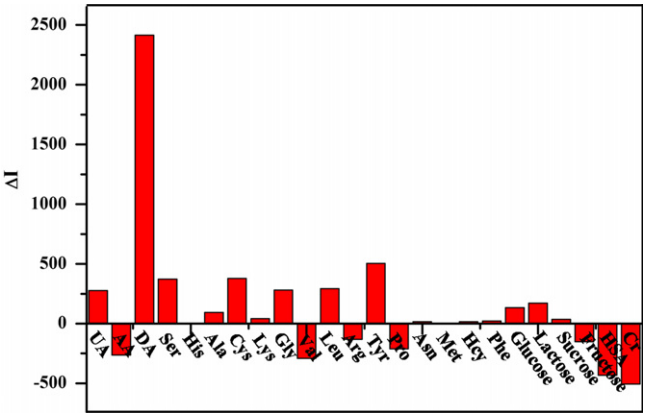

Fig. 7. Fluorescence changes of ZnO QDs with different guest molecules. The concentrations of all guest molecules are 1 μM.

Table 1
Results for the determination of DA in human serum samples.

Serum sample	Spiked (μM)	Measured (μM) (mean ± standard deviation, $n=3$)	Recovery (%) (mean ± standard deviation, $n=3$)
Sample 1	0.00	nd[a]	
	2.00	2.05 ± 0.05	102.50 ± 2.50
	3.00	3.06 ± 0.12	102.00 ± 4.00
	4.00	3.97 ± 0.02	99.25 ± 0.50
Sample 2	0.00	nd	
	2.00	2.10 ± 0.07	105.00 ± 3.50
	3.00	3.08 ± 0.04	102.67 ± 1.33
	4.00	4.39 ± 0.05	109.75 ± 1.25

[a] Not detected.

Table 2
Comparison of different analytical methods for dopamine detection.

Methods	Limit of detection (μM)	Linear range (μM)	References
Colorimetry	0.54–5.4	0.36	[42]
Chemiluminescence	0.57–13	0.18	[43]
Electrochemistry	0.40–374	0.13	[44]
Electrochemiluminescence	0.50–19	0.10	[45]
Fluorescence	0.25–50	0.094	[32]
Fluorescence	0.30–50	0.01	[46]
Fluorescence	0.05–10	0.012	This work

4. Conclusions

In this work, a very sensitive and selective fluorescent method to detect DA using APTES-capped ZnO QDs has been developed, and the involving fluorescence quenching mechanism has also been proposed. The results showed that the DA molecules were adsorbed on QDs surface and electron transfer from photoexcited QDs to oxidized dopamine–quinone resulting in significant fluorescence quenching. Based on this, we successfully developed a simple label-free ZnO QDs based fluorescent probe for selective and sensitive detection of DA in serum samples. The detection limit was 12 nm ($n=3$) and the linear relationship was 0.05–10 μM. To date, sensing of DA in serum using fluorescent ZnO QDs has not been reported. Therefore, this work provided the first example for sensitive sensing of DA in biological fluids using the fluorescent property of ZnO QDs, which may open a new door to detect small biomolecules and metal ions based on the fluorescent property of ZnO QDs.

Acknowledgements

Authors acknowledge the financial support for this project from the National Natural Science Foundation of China [No. 21075084 & No. 21105068].

References

[1] D. Segets, J. Gradl, R.K. Taylor, V. Vassilev, W. Peukert, ACS Nano 3 (2009) 1703–1710.
[2] A. Asok, M.N. Gandhi, A.R. Kulkarni, Nanoscale 4 (2012) 4943–4946.
[3] H.M. Xiong, D.G. Shchukin, H. Möhwald, Y. Xu, Y.Y. Xia, Angew. Chem. Int. Ed. 48 (2009) 2727–2731.
[4] Z.L. Wang, J.H. Song, Science 312 (2006) 242–246.
[5] X.Y. Xu, C.X. Xu, Z.L. Shi, C. Yang, B. Yu, J. Appl. Phys. 111 (2012) 083521.
[6] H.M. Xiong, D.P. Liu, Y.Y. Xia, J.S. Chen, Chem. Mater. 17 (2005) 3062–3064.
[7] D.C. Look, D.C. Reynolds, C.W. Litton, R.L. Jones, D.B. Eason, G. Cantwell, Appl. Phys. Lett. 81 (2002) 1830–1832.
[8] A. Aboulaich, C.M. Tilmaciu, C. Merlin, C. Mercier, H. Guilloteau, G. Medjahdi, R. Schneider, Nanotechnology 23 (2012) 335101.
[9] Q. Yuan, S. Hein, R.D.K. Misra, Acta Biomater. 6 (2010) 2732–2739.
[10] H.M. Xiong, Y. Xu, Q.G. Ren, Y.Y. Xia, J. Am. Chem. Soc. 130 (2008) 7522–7523.
[11] X.S. Tang, E.S.G. Choo, L. Li, J. Ding, J.M. Xue, Chem. Mater. 22 (2010) 3383–3388.
[12] S. Panigrahi, A. Bera, D. Basak, Appl. Phys. Lett. 1 (2009) 2408–2411.
[13] N.R. Jana, H.H. Yu, E.M. Ali, Y.G. Zheng, J.Y. Ying, Chem. Commun. (2007) 1406–1408.
[14] H.R. Tang, Y.M. Li, C.B. Zheng, J. Ye, X.D. Hou, Y. Lv, Talanta 72 (2007) 1593–1597.
[15] C.Y. Jiang, X.W. Sun, G.Q. Lo, D.L. Kwong, J.X. Wang, Appl. Phys. Lett. 90 (2007) 263501.
[16] L.Y. Zhang, L.W. Yin, C.X. Wang, N. Lun, Y.X. Qi, Appl. Phys. Lett. 2 (2010) 1769–1773.
[17] P.Y. Cai, H.J. Song, L.C. Zhang, Y. Lv, Sens. Actuators, B 173 (2012) 93–99.
[18] J. Zhang, R. Zhang, L.H. Zhao, S.Q. Sun, Cryst. Eng. Commun. 14 (2012) 613–619.
[19] Y.L. Wu, C.S. Lim, S. Fu, A.I.Y. Tok, H.M. Lau, F.Y.C. Boey, X.T. Zeng, Nanotechnology 18 (2007) 215604.

[20] D.L. Robinson, A. Hermans, A.T. Seipel, R.M. Wightman, Chem. Rev. 108 (2008) 2554–2584.
[21] S. Nikolaus, C. Antle, H.W. Muller, Behav. Brain Res. 204 (2009) 1–31.
[22] S.Y. Yi, H.Y. Chang, H. Cho, Y.C. Park, S.H. Lee, Z.U. Bae, J. Electroanal. Chem. 602 (2007) 217–225.
[23] O. George, M.L. Moal, G.F. Koob, Physiol. Behav. 106 (2012) 58–64.
[24] L.L. Li, H.Y. Liu, Y.Y. Shen, J.R. Zhang, J.J. Zhu, Anal. Chem. 83 (2011) 661–665.
[25] Q. Liu, X. Zhu, Z.H. Huo, X.L. He, Y. Liang, M.T. Xu, Talanta 97 (2012) 557–562.
[26] Y.S. Zhao, S.L. Zhao, J.M. Huang, F.G. Ye, Talanta 85 (2011) 2650–2654.
[27] L. Liu, S.J. Li, L.L. Liu, D.H. Deng, N. Xia, Analyst 137 (2012) 3794–3799.
[28] R.P.H. Nikolajsen, A.M. Hansen, Anal. Chim. Acta 449 (2001) 1–15.
[29] L.H. Zhang, N. Teshima, T. Hasebe, M. Kurihara, T. Kawashima, Talanta 50 (1999) 677–683.
[30] Y. Ma, C. Yang, N. Li, X.R. Yang, Talanta 67 (2005) 979–983.
[31] D. Seto, T. Maki, N. Soh, K. Nakano, R. Ishimatsu, T. Imato, Talanta 94 (2012) 36–43.
[32] J.L. Chen, X.P. Yan, K. Meng, S.F. Wang, Anal. Chem. 83 (2011) 8787–8793.
[33] Y.Z. Chen, J. Yang, X.M. Ou, X.H. Zhang, Chem. Commun. 48 (2012) 5883–5885.
[34] L.H. Zhao, R. Zhang, J. Zhang, S.Q. Sun, Cryst. Eng. Commun. 14 (2012) 945–950.
[35] Y.S. Fu, X.W. Du, S.A. Kulinich, J.S. Qiu, W.J. Qin, R. Li, J. Sun, J. Liu, J. Am. Chem. Soc. 129 (2007) 16029–16033.
[36] B. Tang, L.H. Cao, K.H. Xu, L.H. Zhuo, J.C. Ge, Q.L. Li, L.J. Yu, Chem. Eur. J. 14 (2008) 3637–3644.
[37] Z.Z. Chen, X.L. Ren, X.W. Meng, Y.Q. Zhang, D. Chen, F.Q. Tang, Anal. Chem. 84 (2012) 4077–4082.
[38] I.L. Medintz, M.H. Stewart, S.A. Trammell, K. Susumu, J.B. Delehanty, B.C. Mei, J.S. Melinger, J.B.B. Canosa, P.E. Dawson, H. Mattoussi, Nat. Mater. 9 (2010) 676–684.
[39] S. Banerjee, S. Kar, J.M. Perez, S. Santra, J. Phys. Chem. C 113 (2009) 9659–9663.
[40] R. Gill, R. Freeman, J.P. Xu, I. Willner, S. Winograd, I. Shweky, U. Banin, J. Am. Chem. Soc. 128 (2006) 15376–15377.
[41] X. Ji, G. Palui, T. Avellini, H.B. Na, C.Y. Yi, K.L. Knappenberger Jr., H. Mattoussi, J. Am. Chem. Soc. 134 (2012) 6006–6017.
[42] Y. Zheng, Y. Wang, X.R. Yang, Sens. Actuators, B 156 (2011) 95–99.
[43] Y.G. Hu, X.X. Li, Z.T. Pang, J. Chromatogr. A 1091 (2005) 194–198.
[44] W. Zhang, Y.Q. Chai, R. Yuan, S.H. Chen, J. Han, D.H. Yuan, Anal. Chim. Acta 756 (2012) 7–12.
[45] R. Cui, Y.P. Gu, L. Bao, J.Y. Zhao, B.P. Qi, Z.L. Zhang, Z.X. Xie, D.W. Pang, Anal. Chem. 84 (2012) 8932–8935.
[46] S.M. Wabaidur, Z.A. ALOthman, M. Naushad, Spectrochim. Acta, Part A 93 (2012) 331–334.